Diagnosis of Crack of Rotor Blades with Genetic Method

YinQuan YU
Mechatronics & Recording Channel Division
A*STAR Data Storage Institute
Singapore
YU_YinQuan@dsi.astar.edu.sg

Chao BI
Mechatronics & Recording Channel Division
A*STAR Data Storage Institute
Singapore
BI_Chao@ dsi.astar.edu.sg

Abdullah Al MAMUN
Department of Electrical and Computer Engineering
National University of Singapore
Singapore

***Abstract*— A methodology of modeling and simulation of rotor blades by using force vibration finite element method is presented. The experiments were conducted with 3D-LDV for verifying the analysis results. The measurements confirm the effectiveness of the modeling and simulation method presented. When Genetic Programming (GP) method and the data base created by the model are used, the accuracy of prediction of crack of the blades generated in the motor/generator operation can be improved.**

Keywords- rotor blades, crack, vibration, 3D-LDV, Genetic Programming

I. INTRODUCTION

Nowadays, climate change is one of the most critical global challenges. Global warming phenomenon is rapidly surfacing in recent years due to emission of greenhouse gases from human activities. Therefore, wind energy, being one of the copiously renewable energy sources, has been, and will be more widely, used in the world. Wind turbine is one of the main candidates for wind energy generation, which are used to harvest the potential energy of wind, available in the range of millions of MW. Reliability of wind turbine is critical to extract this maximum amount of energy from the wind [1]. Structure health monitoring (SHM) of wind turbine is paramount to optimizing its maintenance schedule and avoiding system sudden breakdowns. In the wind turbine operation, the wind force acting on the blade is variable. Therefore the fatigue of turbine blade is unavoidable. This can easily induce cracks in the blades, as well as gradually increase the crack width and depth. In the extreme case, the turbine blade breaks. Therefore, it is indispensable to develop effective approach for structure health monitoring, in particular rotating structure.

Researchers have studied vibration and acoustic signals associated with cracked blades in recent years [2]-[12]. In this paper, the finite element model is built and numerical results are obtained by using commercial software ANSYS 12.0.

The simulation results will be compared with experimental results obtained using a 3D LDV measurement system. Predict formula is derived by using GP (Genetic Programming), and GP results also will be verified with experimental results. The damage grade can be detected based on vibration signals.

II. APPROACH

A. *Finite element analysis (FEA):*

1) mathematical model:

For improving the research efficiency, an electrical fan is used in the analysis. As the structure of the fan is symmetrical, using finite element model, the displacement of the fan can be simplified as:

$$\begin{bmatrix} u_r(r,\theta,z,t) \\ u_\vartheta(r,\vartheta,z,t) \\ u_z(r,\vartheta,z,t) \end{bmatrix} = \sum_{n=0}^{\infty} \begin{bmatrix} \cos(n\vartheta) & 0 & 0 \\ 0 & \sin(n\vartheta) & 0 \\ 0 & 0 & \cos(n\vartheta) \end{bmatrix} \begin{bmatrix} u_{rn}^s(r,z,t) \\ u_{\vartheta n}^s(r,z,t) \\ u_{zn}^s(r,z,t) \end{bmatrix}, \quad (1)$$

where, ϑ, γ and z are three vectors in spherical coordination, respectively. n is the circumferential wave-number and s is symmetrical term with respect to ϑ. For each value of n, the eigenfrequencies and mode shapes are obtained with harmonic beam element.

2) solid & Ansys mode

The software, Solidworks/Ansys, is used for the modeling and simulation of the fan. In the research, the 3D geometry model is composed to describe the fan blades, electrical motor with slide bearing and fan frame, as it is shown in Fig. 1.

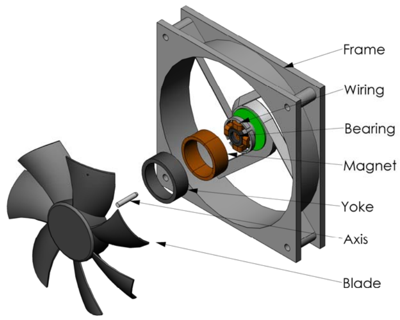

Figure 1. Fan 3D structure

The FEM model is constructed with hexagonal brick-type element and final mesh is applied around crack edges.

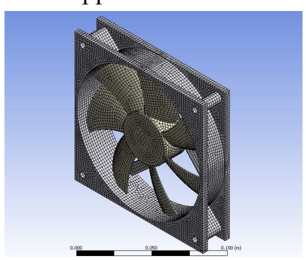

Figure 2. Fan simulation 3D model

In the research, a wind speed meter is used to measure front and rear side wind speed when the fan is running at full speed. The pressure difference ∇P between front and rear sides of the rotating fan can be obtained from the equation below:

$$\nabla P = \frac{1}{2}\rho\left(v_1^2 - v_2^2\right), \quad (2)$$

where v_1 and v_2 are the speeds of front and rear side respectively and ρ is the density of air .

The air density ρ is $1.237\, kg/m^3$, v_1 and v_2 measured are 3m/s and 1.7m/s respectively. So, based on above equation, ∇P is 3.8pa. This pressure will be added on blade front surface as excitation force during dynamics Simulation.

Resonance frequency and amplitude in the X, Y and Z directions can be obtained respectively by using Fourier analysis and the results are show in Fig. 3, Fig. 4, and Fig. 5 respectively:

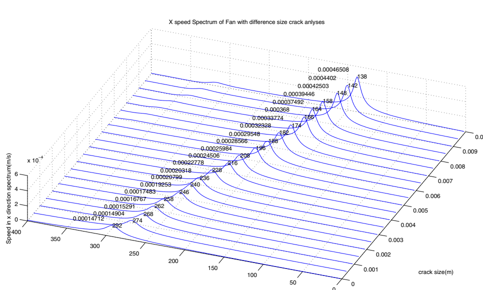

Figure 3. Vibration velocity in X direction with difference crack size (0-10mm on blade rhizine)

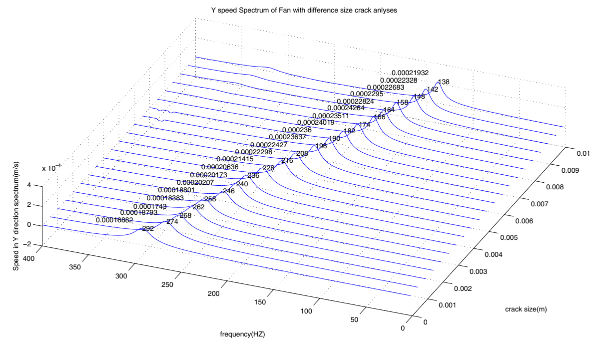

Figure 4. Vibration velocity in Y direction with difference crack size (0-10mm on blade rhizine)

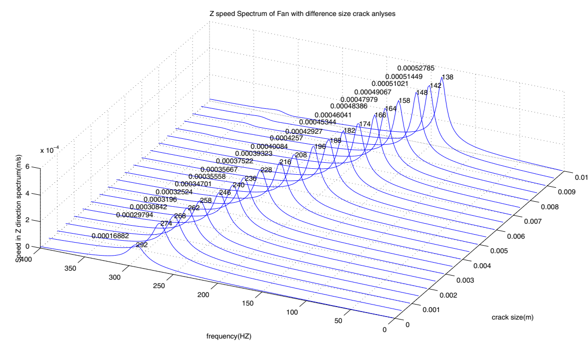

Figure 5. Vibration velocity in Z direction with difference crack size (0-10mm on blade rhizine)

TABLE I. Resonance speed amplitude in X direction and frequency with difference crack size

Crack Size(mm)	Resonance Frequency(HZ)	Maximum Speed in X direction when system resonance(m/s)
0.00	292	0.000147121
0.50	274	0.000149039
1.00	268	0.000152906
1.50	262	0.000167671
2.00	258	0.000174826
2.50	246	0.000192528
3.00	240	0.000207988
3.50	236	0.000203176
4.00	228	0.000227778
4.50	216	0.000245060
5.00	208	0.000259845
5.50	196	0.000285656
6.00	188	0.000295480
6.50	182	0.000323000
7.00	176	0.000335110
7.50	166	0.000368004
8.00	164	0.000374920
8.50	158	0.000394465
9.00	148	0.000425034
9.50	142	0.000440201
10.00	138	0.000465082

TABLE II. Resonance speed amplitude in Y direction and frequency with difference crack size

Crack Size(mm)	resonance frequency(HZ)	Maximum Speed in Y direction when system resonance(m/s)
0.00	292	0.000168819
0.50	274	0.000187928
1.00	268	0.000174298
1.50	262	0.000183828
2.00	258	0.000188013
2.50	246	0.000202073
3.00	240	0.000206358
3.50	236	0.000201732
4.00	228	0.000214152
4.50	216	0.000398902
5.00	208	0.000224275
5.50	196	0.000236370
6.00	188	0.000229884
6.50	182	0.000240000
7.00	176	0.000232875
7.50	166	0.000242642
8.00	164	0.000228238
8.50	158	0.000229502
9.00	148	0.000226831
9.50	142	0.000223280
10.00	138	0.000219319

TABLE III. Resonance speed amplitude in Z direction and frequency with difference crack size

Crack Size(mm)	Resonance frequency(HZ)	Maximum Speed in Z direction when system resonance(m/s)
0.00	292	0.000290841
0.50	274	0.000297941
1.00	268	0.000308423
1.50	262	0.000319598
2.00	258	0.000325235
2.50	246	0.000347008
3.00	240	0.000355578
3.50	236	0.000356666
4.00	228	0.000375219
4.50	216	0.000393226
5.00	208	0.000400842
5.50	196	0.000425698
6.00	188	0.000429266
6.50	182	0.000453000
7.00	176	0.000456426
7.50	166	0.000483862
8.00	164	0.000479789
8.50	158	0.000490669
9.00	148	0.000510207
9.50	142	0.000514494
10.00	138	0.000527848

It can be seen that the resonance frequency decreases as the crack size in the blade increases. However, power spectrum of velocity in the x direction does not gradually increase at each crack size as it is a general assumption that the speed spectrum increases when crack size increases. Therefore prediction of crack size cannot be dependent on the spectrum amplitude but instead dependent on resonance frequency shifting. not as an independent document. Please do not revise any of the current designations.

B. *Fan vibration measurement*

1) experimental setup

Fig. 6 shows the experimental setup of the fan air flow induction vibration on the Guzik spin stand [10]. Lodestar DC power supply 8102A drives the blow fan to full speed and air will be blown to the top experimental fan which has difference size crack. Polytec CLV3000 three dimensional Laser Doppler and Vibrometer (3DLDV) and HP 35670A dynamic signal analyzer (DSA) are employed to measure the velocity power spectrum of a point on the cracked fan blade. The distance between the measured point and axis of fan is 100mm.

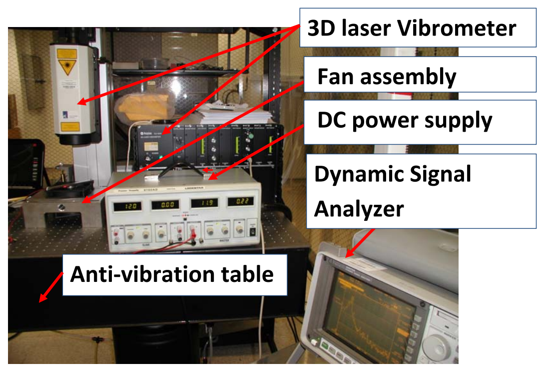

Figure 6. Air-induction measurement setup

2) vibration measurement result

Fig. 7, Fig. 8, Fig. 9 shows the x, y, z direction velocity spectrums of the blade with difference crack size respectively.

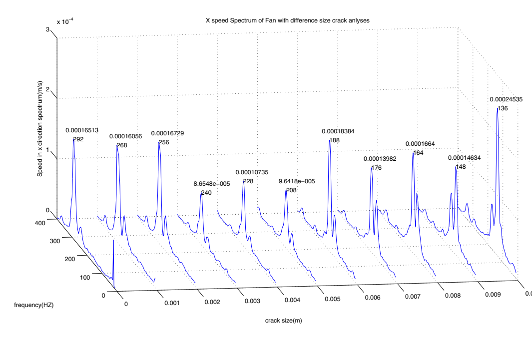

Figure 7. Speed Spectrum in x direction with difference crack size on blade

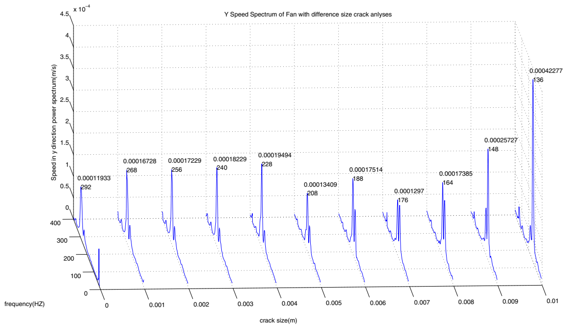

Figure 8. Speed Spectrum in y direction with difference crack size on blade

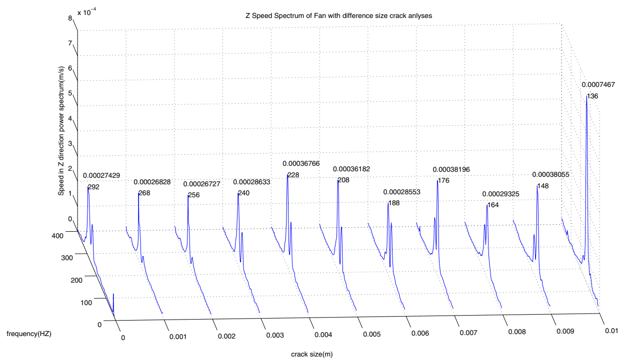

Figure 9. Speed Spectrum in z direction with difference crack size on blade

The experimental resonance speed and resonance frequency in x, y, and z direction with different crack sizes can be obtained from Fig. 7, Fig. 8, Fig. 9 and listed in below Table IV, Table V, Table VI respectively.

TABLE IV. X direction resonance data

Crack Size(mm)	resonance frequency	Maximum Speed in X direction when system resonance(m/s)
0.00	292	0.00016513
1.00	268	0.000160560
2.00	256	0.000167290
3.00	236	0.000086548
4.00	228	0.000107350
5.00	208	0.000096418
6.00	188	0.000183840
7.00	176	0.000139820
8.00	164	0.000166400
9.00	148	0.000146340
10.00	136	0.000245350

TABLE V. Y direction resonance data

Crack Size(mm)	resonance frequency	Maximum Speed in Y direction when system resonance(m/s)
0.00	292	0.00011933
1.00	268	0.000167280
2.00	256	0.000172290
3.00	236	0.000182290
4.00	228	0.000194940
5.00	208	0.000134090
6.00	188	0.000175140
7.00	176	0.000129700
8.00	164	0.000173850
9.00	148	0.000257270
10.00	136	0.000422770

TABLE VI. Z direction resonance data

Crack Size(mm)	resonance frequency	Maximum Speed in Z direction when system resonance(m/s)
0.00	292	0.00027429
1.00	268	0.000268280
2.00	256	0.000267270
3.00	236	0.000286330
4.00	228	0.000367660
5.00	208	0.000361820
6.00	188	0.000285530
7.00	176	0.000381960
8.00	164	0.000293250
9.00	148	0.000380550
10.00	136	0.000746700

It can be seen that experimental frequency results in Fig. 7, Fig. 8, Fig. 9 and Table IV, Table V, Table VI are agreeable with simulation frequency results in Fig. 3, Fig. 4, Fig. 5 and Table I, Table II, Table III; However, the speed spectrum is not consistent in both simulation as well as experimental results. Therefore, it is reasonable to use resonance frequency to predict crack size using genetic programming.

C. Genetic Programming for search and regression

Genetic Programming evolves computer programs, traditionally represented in memory as tree structures. Trees can be easily evaluated in a recursive manner. Every tree node has an operator function and every terminal node has an operand, making mathematical expressions easy to evolve and evaluate. Thus, traditionally GP favors the use of programming languages that naturally embody tree structures [12] .An embryo specifies the starting roots of the developmental growth process. Each embryo will have one or more modifiable sits to allow further growth. GP has terminal set and function set. The main difference between terminal set with function set is the former can only be leaf node and without requiring any child nodes or arguments, while latter are not leaf nodes. Fitness function is used to compute each generation design's "goodness" or "fitness". Fitness function can be defined by user knowledge based formula equation which one or several criterions in which the weighting factors have to be carefully selected can be considered.

GPLAB is a genetic programming toolbox for MATLAB® initially developed by Sara Silva. It is suitable for symbolic regression problems and easily extendable and customized by the user.

The architecture of GPLAB follows a highly modular and parameterized structure, which different users may use at various levels of depth and insight.

The main modules of GBLAB are GENPOP, GENERATION, and SETVARS. GENPOP module generates the initial population and calculates its fitness based on default or user defined fitness function. GENERATION module creates a new generation of individuals by applying genetic operators such as mutation or crossover to previous population. SETVARS either initializes the parameters with the default values or updates them with the user settings.

Terminal set: 'X1', 'rand', and '100'

Terminal condition: Maximum generation reached

Function set: plus (+), minus (-), times (*) and other protected function as Table VII:

Table VII Protected function using MATLAB®

Protected function	MATLAB function	Input arguements	Output arguement
Division	mydivide	a,b	a (if b=0) a/b(otherwise)
Square root	mysqrt	a	0 (if a<=0) sqrt(a) (otherwise)
Power	mypower	a,b	a^b (if a^b is a valid non-complex number) 0 (otherwise)
Natural logarithm	mylog	a	0 (if a=0) log(abs(a))(otherwise)
Base 2 logarithm	Mylog2	a	0 (if a=0) log2(abs(a))(otherwise)
Base 10 logarithm	Mylog10	a	0 (if a=0) log10(abs(a))(otherwise)

Fitness Function

Fitness function is defined as the minimum value between actual value and the predicted value. During the programming calculation process, the new generation population should be better than previous population which means their fitness value will be lower than previous.

Fitness=min (abs (predicted result-expected result))

D. Application GPLAB in experimental results and discussion

Twenty sets of experimental frequency which obtained will be using as input data and the crack size will be used as desired output data.

GPLAB parameter is set as below for running GPLAB programming:

Number of Generation: 100
Population sizes: 1000
Crossover: 0.9
Mutation: 0.1
Selection: roulette
Survival: keep best

Table VIII Simulation data set used to initialize GP

Y data file	X data file	Y data file	X data file
0.00	292	5.50	196
0.50	274	6.00	188
1.00	268	6.50	182
1.50	262	7.00	176
2.00	258	7.50	166
2.50	246	8.00	164
3.00	240	8.50	158
3.50	236	9.00	148
4.00	228	9.50	142
4.50	216	10.00	136

III. RESULTS & DISCUSSION

GPLAB is a genetic programming toolbox for MATLAB®. Versatile, generalist and easily extendable, it can be used by all types of users, from the layman to the advanced researcher.[12] After running GPLAB 100 generation, one good solution has already been found and is shown Fig. 10. The performance of this model is shown Fig. 11.

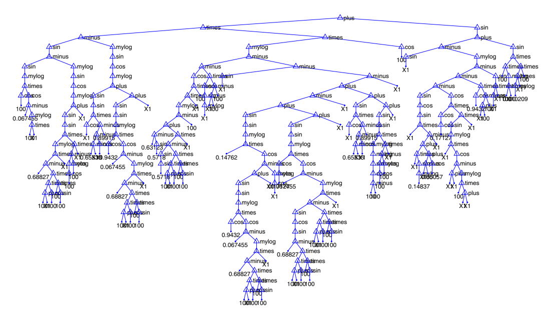

Figure 10. The best solution of the formula

Formula=plus(times(minus(sin(minus(sin(mylog(times(cos(100),cos(minus(0.067455,mylog(times(100,X1))))))),mylog(sin(cos(mylog(plus(sin(sin(times(mylog(times(minus(0.68827,times(times(plus(100,X1),cos(100)),times(100,sin(100)))),X1)),times(minus(mylog(cos(100)),cos(100)),X1)))),X1))))))),mylog(sin(cos(mylog(plus(sin(sin(times(cos(X1),minus(minus(minus(0.65535,X1),cos(X1)),0.89915)))),plus(sin(sin(mylog(times(cos(0.9432),cos(minus(0.067455,mylog(times(minus(0.68827,times(times(plus(100,X1),cos(100)),times(100,sin(100)))),X1)))))))),X1))))))),times(mylog(minus(minus(cos(times(times(mylog(minus(plus(minus(0.63123,sin(0.5718)),times(minus(sin(sin(0.5718)),times(times(plus(100,X1),cos(100)),times(100,sin(100)))),X1)),100)),X1),100)),times(cos(sin(mylog(X1))),minus(plus(X1,100),100))),minus(sin(X1),minus(plus(minus(plus(sin(sin(mylog(times(0.14762,cos(minus(plus(sin(sin(mylog(times(cos(0.9

432),cos(minus(0.067455,mylog(times(minus(0.68827,times(times(plus(100,X1),cos(100)),times(100,sin(100)))),X1)))))))),X1),mylog(cos(X1))))))))),plus(sin(sin(mylog(times(cos(cos(0.17127)),cos(minus(0.067455,mylog(times(minus(sin(cos(sin(minus(0.68827,times(times(plus(100,X1),cos(100)),times(100,sin(100))))))))),times(times(plus(100,X1),cos(100)),times(100,sin(100)))),X1)))))))))),X1)),X1),plus(sin(times(cos(X1),minus(minus(minus(0.65535,X1),cos(X1)),0.89915))),plus(sin(sin(times(mylog(mylog(sin(cos(minus(100,100))))),times(minus(mylog(cos(100)),cos(100)),X1)))),X1))),X1)))),cos(100))),sin(plus(minus(sin(X1),mylog(minus(minus(minus(sin(cos(sin(times(X1,minus(plus(times(X1,sin(mylog(0.14837))),plus(plus(X1,100),cos(0.65057))),X1)))))),cos(times(cos(cos(0.17127)),times(sin(mylog(times(X1,cos(minus(plus(X1,X1),mylog(times(100,plus(X1,X1)))))))),X1)))),times(cos(0.9432),minus(plus(X1,100),100))),sin(times(cos(X1),X1))))),sin(times(times(100,mylog(times(100,100))),times(times(mylog(0.010209),X1),100))))))

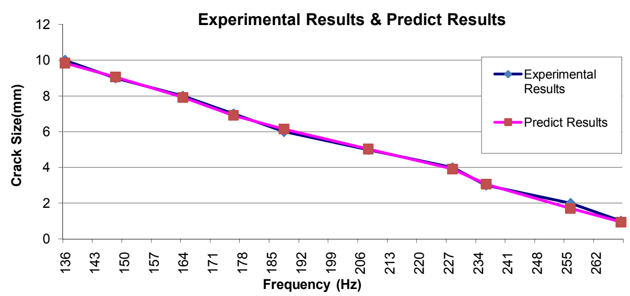

Figure 11. Predict results vs experimental results in Matlab®

The fitness function value result is tabulated in Fig. 12, demonstrating the efficiency of the genetic programming approach. To obtain this result, the program ran in P-IV 2.1GHZ for 38 hours. It took Genetic programming 100 generation to evolve it.

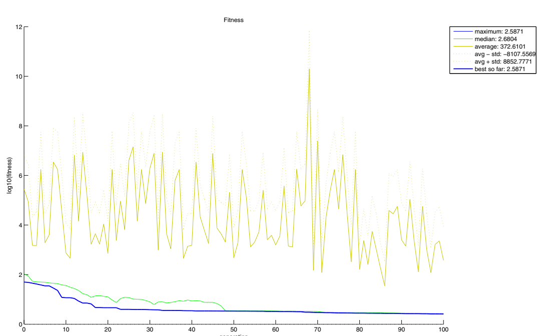

Figure 12. Fitness history for predict formula derived

Fig. 12 shows fitness gradually decrease with generation, which means predict cracks size closes with actual experimental results when GP generation is increased.

IV. CONCLUSION

This paper uses the simulation tool Ansys to first build the model and later calculate the dynamic response with different crack size. Resonance frequency change due to changes in stiffness matrix with difference crack sizes is demonstrated. A new methodology, genetic programming (GP), is used to calculate damage formula depending on the resonance frequency. Using the formula, the future crack size can be predicted in accordance to the resonance frequency.

REFERENCES

[1] Condition monitoring and fault detection of wind turbines and related algorithms: A review Z. Hameeda, Y.S. Honga, Y.M. Choa, S.H. Ahnb,_, C.K. Songc Renewable and Sustainable Energy Reviews 13 (2009) 1–39

[2] Variation in the stability of a rotating blade disk with a local crack defect Bo-Wun Huang, Jao-Hwa Kuang, Journal of Sound and Vibration 294 (2006) 486–502

[3] The influence on coupling vibration of a rotor system due to a mistuned blade length Yi-Jui Chiu, Shyh-Chin Huang International Journal of Mechanical Sciences 49 (2007) 522–532

[4] Effect of number of blades distribution of cracks on vibration localization in a cracked pre-twisted blade system Bo-Wun HUANG International Journal of Mechanical Sciences 48 (2006) 1-10

[5] Crack induced vibration localization in simplified blade-disk structures X.Fanf, J.Tang,E.Jordan,K.D.Murphy Journal of sound and vibration 291 (2006) 395-418

[6] Helicopter rotor blade frequency evolution with damage growth and signal processing Niranjan Roy, Ranjan Ganguli Journal of sound and vibration 283 (2005) 821-851

[7] The effect of blade crack on mode localization in rotating bladed disks J.H.KUANG and B.W.HUANG Journal of sound and vibration (1999) 227(1) 85-103

[8] Damage detection of cracked thick rotating blades by spatial wavelet based approach Chih-ChiehChang, Lien-Wen Chen Applied Acoustics 65(2004)1095-1111

[9] Monitoring low cycle fatigue damage in turbine blade using vibration characteristics Sandeep Kumer, Niranjan Roy, Ranjan Ganguli mechanical systems and signal processing 21 (2007) 480-501

[10] Acoustic resonances and blade vibration in axial flow compressors R.Parker Journal of sound and vibration (1984) 92(4)529-539

[11] Damage prediction of rotating blades using displacement residuals Journal of sound and vibration 316(2008) 25-31

[12] GPLAB A Genetic Programming Toolbox for MATLAB Sara Silva ECOS - Evolutionary and Complex Systems Group University of Coimbra Portugal Version 3 April 2007